Regulation of the Wild-Type and Y1235D Mutant Met Kinase Activation

Cinzia Cristiani,*,‡ Luisa Rusconi,‡ Rita Perego,‡ Nikolaus Schiering,§,|| Henryk M. Kalisz,‡ Stefan Knapp,§,⊥ and Antonella Isacchi‡

Biology and Chemistry Departments, Nerviano Medical Sciences, Viale Pasteur 10, 20014 Nerviano (Milan), Italy

Received June 28, 2005; Revised Manuscript Received August 29, 2005

ABSTRACT: Met receptor tyrosine kinase plays a crucial role in the regulation of a large number of cellular processes and, when deregulated by overexpression or mutations, leads to tumor growth and invasion. The Y1235D mutation identified in metastases was shown to induce constitutive activation and a motile-invasive phenotype on transduced carcinoma cells. Wild-type Met activation requires phosphorylation of both Y1234 and Y1235 in the activation loop. We mapped the major phosphorylation sites in the kinase domain of a recombinant Met protein and identified the known residues Y1234 and Y1235 as well as a new phosphorylation site at Y1194 in the hinge region. Combining activating and silencing mutations at these sites, we characterized in depth the mechanism of activation of wild-type and mutant Met proteins. We found that the phosphotyrosine mimetic mutation Y1235D is sufficient to confer constitutive kinase activity, which is not influenced by phosphorylation at Y1234. However, the specific activity of this mutant was lower than that observed for fully activated wild-type Met and induced less phosphorylation of Y1349 in the signaling site, indicating that this mutation cannot entirely compensate for a phosphorylated tyrosine at this position. The Y1194F silencing mutation yielded an enzyme that could be activated to a similar extent as the wild type but with significantly slower activation kinetics, underlying the importance of this residue, which is conserved among different tyrosine kinase receptors. Finally, we observed different interactions of wild-type and mutant Met with the inhibitor K252a that may have therapeutic implications for the selective inhibition of this kinase.

Met tyrosine kinase is a high-affinity transmembrane receptor for the hepatocyte growth factor (HGF)[1] (*1*), which was originally identified as an oncogene (*2*). Stimulation of Met by HGF initiates numerous physiological processes, including cell proliferation, scattering, morphogenic differentiation, angiogenesis, wound healing, tissue regeneration, and embryological development (*3*, *4*). Deregulation of Met and/or HGF, Met overexpression, and Met mutations are implicated in uncontrolled cell proliferation and survival and play a key role in early-stage tumorigenesis and metastasis (*5*−*8*), making Met an interesting target for anticancer drug development (*9*). Recent data demonstrating the suppression of cancer cell proliferation, survival, and invasion upon inhibition of Met binding to HGF and Met receptor dimerization (*10*, *11*) confirm the relevance of Met in neoplasia and provide further proof of concept for the development of small-molecule compounds for antineoplastic therapy.

Activation of Met occurs through dimerization upon binding of HGF to its extracellular region (*12*, *13*), followed by autophosphorylation of the highly conserved residues Y1234 and Y1235 in the activation loop (A loop) (*14*−*16*). Substitution of Y1234 and Y1235 in the A loop with phenylalanine yields an inactive kinase and completely abolishes Met biological response to the ligand (*15*). Kinase activation by autophosphorylation leads to the subsequent phosphorylation of Y1349 and Y1356 in the C-terminal multifunctional docking site, resulting in the activation of Met signaling (*16*) through the recruitment of a variety of SH2-containing signal transducers and effectors (*4*, *17*, *18*).

Activating germ-line mutations in the Met tyrosine kinase domain were detected in the majority of hereditary papillary renal carcinomas (*20*, *21*) and in a gastric cancer (*22*), whereas somatic mutations have been found in a small proportion of sporadic papillary kidney carcinomas (*23*), some childhood hepatocellular carcinoma (*24*), and different carcinoma metastases (*25*, *26*). Modeling studies suggest that activating mutations observed in Met might either destabilize the inactive conformation or stabilize the active conformation of the enzyme (*27*). Some of these mutations, such as D1228H, D1228N, and M1250T, have been shown to lower the threshold for kinase activation by overcoming the need for phosphorylation of Y1234 (*28*), leading to uncontrolled cell proliferation and tumorigenesis.

* To whom correspondence should be addressed: E-mail: cinzia.cristiani@nervianoms.com. Telephone: +39-0331-581278. Fax: +39-0331-581267.

‡ Biology Department.

§ Chemistry Department.

|| Current address: Novartis Pharma AG, Novartis Institutes for BioMedical Research Basel, Protease Platform, WKL-127.P.72, CH-4002 Basel, Switzerland.

⊥ Current address: Structural Genomics Consortium (SGC), University of Oxford, Botnar Research Centre, Oxford OX3 7LD, U.K.

[1] Abbreviations: HGF, hepatocyte growth factor; A loop, activation loop; HNSCC, head and neck squamous cell carcinoma; PCR, polymerase chain reaction; GST, glutathione *S*-transferase; DTT, dithiothreitol; TFA, trifluoroacetic acid; LC/ESI−MS, liquid chromatography/electrospray ionization mass spectrometry; MALDI−MS, matrix-assisted laser desorption ionization mass spectrometry; IMAC, immobilized metal-affinity chromatography; CD, circular dichroism; PBS, phosphate-buffered saline; ITC, isothermal titration calorimetry.

10.1021/bi051242k CCC: $30.25
Published on Web 10/04/2005

The Y1235D mutation identified in metastases from head and neck squamous cell carcinoma (HNSCC) was found to induce constitutive Met activation and conferred a motile-invasive phenotype on transduced carcinoma cells (*25*, *26*). Epithelial cells expressing a TRK/Met chimera harboring the Y1235D mutation grew in an anchorage-independent manner and were able to invade *in vitro* reconstituted basal membranes. These properties were detected in the absence of the ligand and were enhanced upon receptor dimerization (*25*).

Combining silencing and activating mutations of key residues in the Met kinase domain, we were able to identify the FFD (Y1194F, Y1234F, and Y1235D) mutant that can be produced in insect cells as a soluble, homogeneous, and unphosphorylated form of the Met kinase domain, retaining enzymatic activity. Recently, we published the crystal structure of the Met FFD mutant alone and in complex with the Staurosporin analogue K-252a (*29*). This study has provided structural information for the Met kinase domain harboring a mutation found in human cancer (Y1235D) and allowed mapping of other cancer-related mutations, contributing to an understanding of the mechanism of activation observed in different oncogenic mutants.

Here, we report the biochemical approach that allowed us to obtain the Met derivative suitable for crystallographic studies and an in depth functional characterization of the role of individual residues that are mutated in the FFD derivative. This work identifies residues 1194, 1234, and 1235 as major phosphorylation sites in the Met kinase domain and analyses their relevance for wild-type Met enzymatic activation. These results also contribute to the elucidation of the molecular basis for the biological phenotype of Met mutants harboring the Y1235D and Y1194F mutations (*25*, *26*, *30*).

MATERIALS AND METHODS

Cloning and Expression. Human cDNA was used as a template for amplification by polymerase chain reaction (PCR) of the full-length cytoplasmic form of Met (residues 958−1390). The following primers, containing a *Bam*HI restriction site, were used: forward (fw) 5′-CCATCTGGATCCAGAAAGCAAATTAAAGATCTGGG-3′; reverse (rv) 5′-CATAGGGATCCTCTAGACTATGATGTCTCCCAGAAGGA-3′. The PCR product was cloned into pVL1393 (Pharmingen), a transfer vector for the baculovirus expression system. Glutathione *S*-transferase (GST) and a PreScission cleavage site, obtained from the pGEX-6P vector (Amersham Biosciences), were inserted before the multiple-cloning site, and the GST open-reading frame was modified to include a Kozak sequence at the ATG initiation codon.

The construct designed following limited proteolysis (residues 1023−1360) was cloned into the same modified vector using the full-length cDNA as a template for PCR. The forward primer (5′-CCATCTGGATCCCAAGTGCAGTATCCTCTGAC-3′) contained a *Bam*HI restriction site; the reverse primer (5′-CCATCTGAATTCTCATTTTACGTTCACATAAGTAGCG-3′) contained an *Eco*RI site. Point mutations were generated using the QuickChange Site-Directed Mutagenesis Kit (Stratagene). Two complementary oligonucleotides phosphorylated at the 5′ end and containing the desired base alterations flanked by unmodified nucleotides were synthesized for each tyrosine substitution. After PCR and digestion with *Dpn*I, the treated DNA was transformed into XL1-Blu supercompetent cells and minipreps (Qiagen) were prepared from different colonies to check the DNA sequence. The following oligonucleotides were used to create the mutants: *Y1194F-fw*, 5′-GGCATGAAATTTCTTGCAAGCTTT-3′; *Y1194F-rv*, 5′-TTTGCTTGCAAGAAATTTCATGCC-3′; *Y1235D-fw*, 5′-ATGTATGATAAATACGATAGTGTACACAACAAAACA-3′; *Y1235D-rv*, 5′-TGTTTTGTTGTGTACACTATCGTATTCTTTATCATA-3′; *Y1234F-fw*, 5′-GACATGTATGATAAAGAATCCGATAGTGTACACAACAAA-3′; and *Y1234F-rv*, 5′-TTTGTTGTGTACACTATCGAATCCTTTATCATACATGTC-3′.

Sf9 or Sf21 insect cells (Invitrogen) were cotransfected with 3 μg of purified plasmid and 1 μg of virus DNA (BaculoGold Transfection Kit, Pharmingen). After the third viral amplification, a virus titer of $5 \times 10^7-10^8$ pfu/mL was obtained. Proteins were produced in High-five cells (Invitrogen) infected with a multiplicity of infections (MOI) of 1 or 2. Different infection times (48 and 72 h) and temperatures (21 and 27 °C) were used to optimize soluble protein production. Harvested cells were pelleted at 1200*g* for 10 min.

Protein Purification. A total of 10×10^9 cells were resuspended in 1 L of 50 mM Tris at pH 7.4, 150 mM NaCl, 10% glycerol, 20 mM dithiothreitol (DTT), and "complete" protease inhibitor cocktail (10 tablets/L, Roche) and lysed by liquid extrusion with a Gaulin homogenizer (Niro Soavi, Italy). After centrifugation at 20000*g* for 20 min, the supernatant was loaded onto a column containing 100 mL of Glutathione Sepharose. The column was washed with 10 column volumes of 50 mM Tris at pH 7.4, 150 mM NaCl, 10% glycerol, and 3 mM DTT (washing buffer). The resin was then resuspended in washing buffer containing 1.5 mL of PreScission protease (3000 units) (Amersham Biosciences) and left overnight at 4 °C. The cleaved protein was then recovered, and the resin was washed with 150 mL of washing buffer. The pool was subjected to gel filtration on a Superdex 200 column equilibrated in 50 mM Tris at pH 7.4, 150 mM NaCl, and 3 mM DTT.

In Vitro Dephosphorylation and Autophosphorylation. Dephosphorylation was performed by incubation of the affinity-purified protein with alkaline phosphatase (Calbiochem) (400 units of phosphatase/mg of protein, in the presence of 1 mM $MgCl_2$, for 1 h at 30 °C and pH 7.4) or λ phosphatase (NEB) (10 000 units phosphatase/mg of protein, in the presence of 4 mM $MnCl_2$ and 5 mM DTT, at pH 7.4). The protein was then purified by gel filtration on a Superdex 200 column (Amersham) in phosphate-buffered saline (PBS) [isothermal titration calorimetry (ITC) studies] or Tris (specific activity) buffer as described above. Autophosphorylation was performed by incubating the purified protein at a concentration of 0.7−1.0 mg/mL (20−30 μM) with 10 mM ATP and 10 mM $MgCl_2$ for 1 h at room temperature. The reaction was stopped by addition of EDTA to a final concentration of 30 mM, and the protein was subjected to gel filtration as described above.

Biochemical Assays. In the activity assay, the proteins were incubated for 15 min at 37 °C in a mixture containing 50 mM Hepes at pH 7.5, 3 mM Mg^{2+}, 3 mM Mn^{2+}, 100 μM ATP, 50 μM gastrin, 1 mM DTT, and 0.05 mg/mL bovine serum albumin. The reaction was stopped by the addition of EDTA to a final concentration of 80 mM. Phosphorylated and unphosphorylated gastrin were separated by injecting 20 μL of the mixture onto a Xterra RP18 HPLC column

(3.5 μm, 4.6 × 50 mm) and eluting at 1 mL/min with a gradient from 14.4 to 45% acetonitrile in 10 mM phosphate at pH 6.5. Specific activity is calculated as the amount (nmol) of gastrin phosphorylated by 1 mg of enzyme/min at 37 °C.

Gel Kinase Assay. The autophosphorylation assay was carried out at room temperature using dephosphorylated Met at two different concentrations (100 nM and 1 μM) suspended in 20 μL of kinase buffer (50 mM Hepes at pH 7.5, 3 mM $MgCl_2$, 3 mM $MnCl_2$, 1 mM DTT, and 3 mM $NaOVO_3$) containing [γ-^{32}P]ATP (2.5 μCi/sample) and 10 μM unlabeled ATP. The reaction was stopped by addition of 10 mM EDTA (final concentration) as well as by Laemmli buffer. Reactions were analyzed using 10% SDS−PAGE and autoradiography of the dried gel.

Mass Spectrometry. Protein preparations were analyzed for full molecular weight determination by liquid chromatography/electrospray ionization mass spectrometry (LC/ESI−MS) using a 1090 LC apparatus coupled through an API−ESI source to a 1946 MSD single quadrupole MS detector (Agilent, Palo Alto, CA). A sample volume containing 10−25 μg of total protein was loaded isocratically onto a Vydac C4 column (2.1 mm ID × 250 mm), and proteins were eluted applying a gradient from 5 to 75% eluent B over 70 min [eluent A, 0.05% trifluoroacetic acid (TFA) in water; eluent B, 0.05% TFA in acetonitrile] at a flow rate of 200 μL/min. Mass spectra were acquired in the 600−2000 *m*/*z* range and deconvoluted using the ChemStation deconvolution software package (Agilent). Deconvolution was mostly performed under limited stringency conditions (envelope cutoff = 0−15%) to maximize the recognition of protein species eluting under the same chromatographic peak but having different phosphorylation levels. Experimental molecular weight values were matched to the expected ones using the protein analysis software Paws (www.proteometrics.com).

Protein enzyme digests were analyzed by matrix-assisted laser desorption ionization mass spectrometry (MALDI−MS) on a Voyager DE-Pro BioSpectrometry Workstation MALDI−TOF mass spectrometer (Applied Biosystems, Foster City, CA) equipped with a N_2 laser (337 nm, 3-ns pulse width, 20-Hz repetition). A total of 0.5 μL of sample was spotted onto the MALDI plate, and 0.5 μL of matrix solution, prepared by dissolving 10 mg of α-cyano-4-hydroxycynnamic acid in a 1:1 water/acetonitrile mixture containing 0.1% TFA, was added. The spot was air-dried at room temperature. The mass spectrometric analysis was performed in reflectron mode by applying an accelerating voltage of 20 kV, a grid voltage of 75%, and a delay time of 200 ns. Spectra were calibrated internally.

Limited Proteolysis. Limited proteolysis was performed on the full-length cytoplasmic domain of Met (residues 958−1390). The following experimental conditions were used: 2 μg of Met were incubated for 20 min at room temperature in a buffer containing 90 mM Tris/HCl at pH 8.5, 4 mM DTT, and 2 mM $CaCl_2$ with increasing amounts of trypsin (0.2−4 μg), in a final volume of 20 μL. The reaction was stopped by boiling the samples in the presence of SDS sample buffer for 5 min and by loading the samples immediately onto a 12% BisTris gel. V8 enzyme titration was carried out under similar conditions, using 50 mM Tris/HCl at pH 7.8 and 10 μM DTT as the buffer and 0.01−3 μg of the enzyme.

Phosphorylation-Site Mapping. Protein samples (50−150 μg) were digested either in solution or in gel with TPCK-treated trypsin (Fluka, Buchs, Switzerland) using a 1:30 E/S ratio for 16 h at 37 °C. The digests were desalted on C18 ZipTips (Millipore, Bedford, MA) and eluted stepwise with acetonitrile (20, 50, and 80%) in 0.2% aqueous TFA. Fractions were analyzed by MALDI−MS, and extensive sequence reconstruction was achieved by matching the MALDI peaks to the molecular weight values of expected tryptic fragments. The spectra were then inspected for peaks showing a +80 shift with respect to the expected value and accounting for possible phosphopeptides. Aliquots of phosphopeptide containing fractions were (a) treated with calf intestine alkaline phosphatase (Sigma, St. Louis, MO, about 0.5 unit/10 μg of peptide digest for 1 h at 37 °C) or recombinant protein tyrosine phosphatase 1b (1 μg/150 μg of peptide digest for 16 h at 4 °C) for phosphate removal and (b) submitted to immobilized metal-affinity chromatography (IMAC) on Fe^{3+}-loaded MC ZipTips (Millipore) for phosphopeptide enrichment according to the protocol of the manufacturer. Both (a) and (b) treated samples were analyzed by MALDI−MS, and their spectra were compared to those of the untreated fractions. The samples from IMAC enrichment were also treated with a phosphatase and re-analyzed by MALDI−MS to confirm the conversion of each phosphopeptide peak to the *m*/*z* value of the parent unmodified peptide.

N-Terminal Sequence Analysis. Samples were run in homogeneous 10 or 12% SDS−PAGE, and after electroblotting (300 mA, 90 min) onto a PVDF membrane and Coomassie staining, the bands of interest were excised and loaded into a 477A or a cLC Procise sequencer (Applied Biosystems).

Circular Dichroism (CD). CD spectra were recorded using an AVIV 215 CD spectrophotometer and software provided by the manufacturer. A cell with a 0.1 cm path length was used. Each spectrum was averaged using two accumulations collected in 1 nm intervals with an averaging time of 10 s. A blank spectrum was subtracted from the averaged data spectra to correct for buffer effects. Spectra were measured in 10 mM sodium phosphate buffer and 20 mM NaCl at 10 °C. Secondary structure content of the spectral data was determined using the self-consistent method and Selcon 3 (*31*).

ITC. Calorimetric measurements were carried out at constant temperatures using a VP-ITC titration calorimeter (MicroCal, Inc.). Samples were extensively dialyzed against PBS (Sigma) and 1 mM DTT. All solutions were carefully degassed before the titrations using equipment provided with the calorimeter. Each titration experiment consisted of a first (2 μL) injection followed by 10 μL injections. Heats of dilution were measured in blank titrations by injecting the ligand (protein in reverse titrations) into the buffer used in the particular experiment and were subtracted from the binding heats. Data were analyzed using a single binding site model implemented in the Origin software package.

Analytical Ultracentrifugation. Sedimentation velocity and equilibrium data were recorded using a Beckman XL-I analytical ultracentrifuge. All data were measured in PBS and 1 mM DTT at 8 °C. Sedimentation equilibrium data were measured using a six-channel centerpiece and an AN-50-TI rotor. Runs were performed at 10 000, 12 000, and 15 000

rpm, and each speed was maintained until no significant difference was observed in scans taken 2 h apart. The measured data were analyzed using a single component model implemented in the Origin. Sednterp was used to calculate partial specific volume and buffer density. Sedimentation velocity data were collected at 50 000 rpm. Sample volumes (400 μL) of a protein concentration of 0.2 mg/mL were loaded into a two-sector centerpiece sample cell. Data were analyzed using dcdtplus (*32*).

Western Blotting. For Western blots, 500 ng of each purified protein was used. Phosphorylation was detected using either an anti-phosphotyrosine antibody (clone 4G10-upstate) or a polyclonal antibody recognizing phosphotyrosine Y1349 (cell signaling technology). Alexa Fluor 680 goat anti-mouse IgG, labeled with far-red fluorescent dye (Molecular Probes−Invitrogen), or IRDye800 conjugated affinity-purified anti-rabbit IgG (H&L) (Rockland, PA) were used as secondary antibodies. The Odyssey Infrared Imaging System (Li-Cor Biosciences) was used for detection.

RESULTS

Production of Recombinant Met Protein. The definition of domain boundaries is a crucial step for the expression of stable and homogeneous protein for biochemical, biophysical, and structural studies. Limited proteolysis was performed on the entire Met cytoplasmic domain to define the most suitable boundaries. Titration with trypsin yielded a stable fragment of about 40 kDa that was mapped to residues 1023−1360 using electrospray mass spectrometry and N-terminal sequencing. A similar result was obtained using V8 protease (data not shown). The identified domain was expressed in baculovirus-infected insect cells. Optimization of the cell culture, cell type, and infection conditions resulted in yields of 5−10 mg of pure protein/10^9 insect cells. Recombinant Met was purified to more than 90% homogeneity using Glutathione Sepharose affinity chromatography. The recombinant wild-type protein was highly phosphorylated, and up to seven phosphorylation species were detected by mass spectrometry (Figure 1A).

Mapping of the Major Phosphorylation Sites. The MALDI spectrum of a digested fraction after phosphopeptide enrichment is shown in the Supporting Information (Figure S1A). The peak with an *m*/*z* value of 1891.1 was mapped to a peptide containing residues 1181−1198 with an additional mass increment of 80 mass units expected for a phosphorylated peptide. Interestingly, the only tyrosine present in this peptide, Y1194, had not been described previously as a phosphorylation site in Met. The remaining two peaks were mapped to the mono- and diphosphorylated forms of fragment 1228−1239 in Met. To confirm the phosphorylation of these peptides, the IMAC-enriched peptide mixture was treated with alkaline phosphatase. The three phosphopeptide peaks disappeared, and concomitantly, two new peaks corresponding to the mass of the unmodified peptide fragments 1181−1198 and 1228−1239 appeared (Figure S1B in the Supporting Information). The enriched diphosphorylated phosphopeptide 1228−1239 contained three tyrosine residues. To understand which tyrosines (Y1230, Y1234, and Y1235) were modified, the total MALDI spectrum was carefully inspected and a shorter phosphopeptide corresponding to the fragment 1233−1239 was also observed. This peptide was found to contain both phosphorylated residues, whereas no phosphorylated counterpart was present in any peptide containing Y1230 (data not shown). Double phosphorylation of the fragment 1233−1239 was confirmed by observed mass shifts of 160 mass units upon treatment with alkaline phosphatase (data not shown). Thus, we identified Y1194, Y1234, and Y1235 as the major phosphorylated sites in the recombinant Met protein kinase domain.

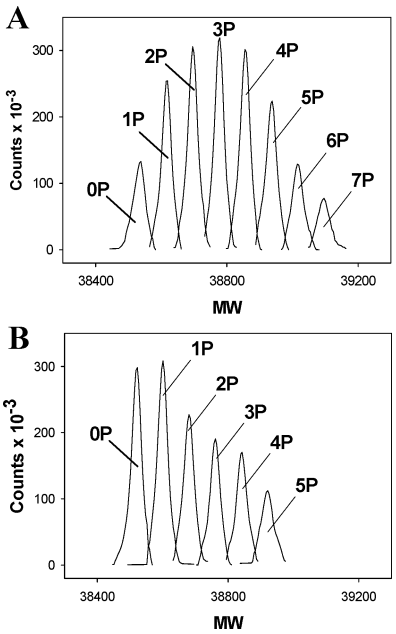

FIGURE 1: Phosphorylation-state analysis of recombinant Met by LC/ESI−MS. (A) YYY Met. (B) FYY Met. The phosphorylation state is indicated for each species (see Table 1 for a comprehensive relative quantitation of the phosphorylated species). The experimental MW values of the unphosphorylated (0P) species of YYY (38 537.6) and FYY (38 521.7) are in close agreement with the expected values (YYY, 38 538.5; FYY, 38 522.5).

Mutagenesis and Biophysical Properties of Met Mutants. To obtain an insight into the function of the three major phosphorylation sites and reduce the overall molecule phosphorylation state, mutants were designed comprising silencing (from Tyr to Phe) mutations at Y1194 and/or Y1234, in combination with the phosphotyrosine mimetic mutation Y1235D found in HNSCC (*25*). Four Met mutants were produced: the single mutants Y1194F (named FYY) and Y1235D (named YYD), the double mutant Y1194F/Y1235D (named FYD), and the triple mutant Y1194F/Y1234F/Y1235D (named FFD). The positions of the mutated residues in the 3D structure of Met (*29*) are shown in Figure 2. Y1194 is located between helix αE at the interface with αC from the N lobe in close proximity to the hinge region of Met, while Y1234 and Y1235 are in the activation loop. The mutants were heterologously expressed in insect cells and purified to more than 90% purity under similar conditions to those used for the wild type (hereafter referred to as YYY) Met.

The YYY Met and the mutants had similar CD spectra, indicating that the overall structural integrity of the protein was not altered by the mutations (Figure S2 in the Supporting Information). Deconvolution of the data using Selcon 3 resulted in the determination of an α-helical and β-sheet content of 31 and 15.9% for YYY Met and 29.3 and 14.9% for the FFD mutant.

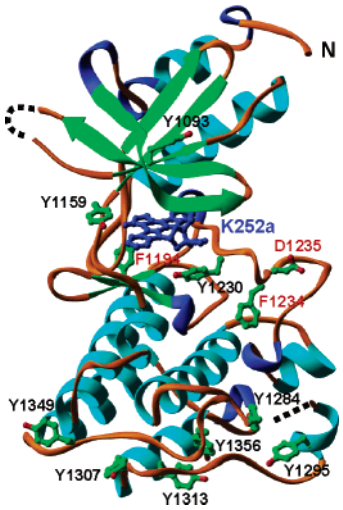

FIGURE 2: Ribbon diagram of the Met FFD K252a complex. The inhibitor (in blue) and tyrosine residues of Met (in green) are shown in a ball-and-stick representation. The three mutated residues (Y1194F, Y1234F, and Y1235D) are highlighted in red. Loop regions that were not defined in the crystal structure are indicated by dotted lines. The picture has been generated using ICM.

Table 1: Phosphorylation States and Specific Activities of Different Forms of Met[a]

group	mutant	specific activity (nmol mg^{-1})	0P%	1P%	2P%	3+P%	phosphates/ molecule
A	YYY	147± 40	8	15	17	60	2.29
	FYY	78 ± 10	22	23	17	38	1.17
	YYD	174 ± 36	95	5			0.05
	FYD	62 ± 5	85	15			0.15
	FFD	60 ± 3	100				0
B	YYY	154 ± 31	69	23	8		0.39
	FYY	91 ± 16	76	24			0.24
	YYD	184 ± 24	100				0
	FYD	58 ± 6	100				0
C	YYY	264 ± 34	8	19	26	47	2.12
	FYY	258 ± 35	2	8	19	71	2.59
	YYD	172 ± 8	0	31	65	4	1.73
	FYD	55 ± 5	0	87	13		1.13

[a] Different forms of Met were characterized for their phosphorylation state and *in vitro* kinase activity directly after purification from insect cells (A), after *in vitro* treatment with alkaline phosphatase (B), and after *in vitro* dephosphorylation followed by preincubation with 10 mM ATP (C). Data represent five independent experiments performed in duplicate. P% = percentage of phosphorylated sites.

Analysis of the mutants by analytical ultracentrifugation showed the recombinant proteins to be monomeric and monodisperse in solution. YYY Met and the four mutants had sedimentation coefficients [s(20,w)] between 2.17 and 2.25 Svedberg units (data not shown). The molecular weights in solution of 39.7, 37.1, and 37.5 kDa for YYY, FYD, and FFD, determined from sedimentation equilibrium experiments, were in good agreement with the expected theoretical molecular weight (data not shown).

Phosphorylation State and Specific Activity of the Different Met Forms. To investigate the relationship between phosphorylation and activity of YYY Met and its mutants, the overall phosphorylation state was analyzed by Western blotting with pan anti-pTyr antibodies and quantified by ESI−MS (Table 1 and Figure 3A). The results obtained by immunoblotting were in good correlation with the total phosphorylation levels determined by ESI−MS. The wild-type YYY and the FYY mutant were expressed as highly phosphorylated proteins (Table 1, group A). While YYY Met was prevalently (60%) phosphorylated on three or more sites, with 2.3 phosphates/molecule, only 38% of the FYY Met was phosphorylated on three or more sites, with an average of 1.2 phosphates/molecule (Table 1, group A, and Figure 1B). In contrast, all expressed proteins containing the Y1235D mutation (FFD, FYD, and YYD) were essentially unphosphorylated, with less than 0.2 phosphates/molecule (Table 1, group A, and Figure 3A).

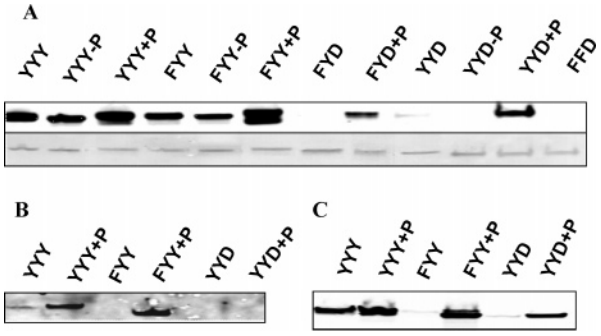

FIGURE 3: Western blot analysis of total and specific phosphorylations of Met and its mutants. Samples of 500 ng of protein were resolved by SDS−PAGE under reducing conditions. (A) Phosphorylation content was determined using pan anti-phosphotyrosine antibodies (upper panel). To control sample loading, proteins were visualized in the gels by staining with Coomassie Brilliant Blue (lower panel). Alkaline phosphatase-treated protein is indicated by "−P" and autophosphorylated protein by "+P". Spot intensity detected by Western blotting corresponded well with the ESI−MS data summarized in Table 1. (B) A-loop phosphorylation of YYY, FYY, and YYD before and after (+P) autophosphorylation, using specific anti-pY1234/Y1235 antibodies. The apparent lack of phosphorylation on Y1234 in the YYD mutant after *in vitro* autophosphorylation can be explained by the lack of recognition of the modified A loop containing the Y1235D substitution. (C) Docking-site activation was analyzed using anti-pY1349 polyclonal antibodies directed against the residues surrounding Y1349 of human Met.

The specific activities of YYY and the four Met mutants after expression in insect cells were tested in an *in vitro* kinase assay using a gastrin peptide as the substrate. Data represent the average of five repeated experiments using two separate protein preparations. Interestingly, the specific activity was not correlated with the overall phosphorylation state of the proteins, because the YYY and YYD proteins demonstrated the highest activities, despite their different phosphorylation states. Instead, the specific activity correlated with the presence of the Y1194F mutation, because the FFD, FYD, and FYY mutants reproducibly demonstrated 2−3-fold lower activity than the YYD and YYY Met proteins (Table 1, group A). Further, the YYD mutant consistently had a slightly higher activity than YYY, in agreement with previously reported data for a Met form harboring the Y1235D mutation and immunoprecipitated from COS-7 transfected cells (*25*).

To investigate whether the observed differences in the specific activities were due to minor but relevant differences in the levels of phosphorylation in the A loop, the proteins were dephosphorylated and then subjected to *in vitro* autophosphorylation. The levels of phosphorylation and the specific activities were measured after each step. The FFD mutant was not included in this and the next experiment, because its activity cannot be modulated by phosphorylation

because of the absence of the major phosphorylation sites (data not shown). Incubation with alkaline phosphatase resulted in the complete dephosphorylation of FYD and YYD. In contrast, despite a significant reduction in the levels of phosphorylation of FYY and YYY, it was not possible to completely dephosphorylate the two proteins and 25−30% of the protein remained phosphorylated, with 0.2−0.4 phosphates/molecule (Table 1, group B, and Figure 3A). Mapping of YYY showed that phosphorylation was located on the phosphopeptide containing Y1234−Y1235. The inability to completely dephosphorylate the proteins was most likely due to the inaccessibility of the phosphorylated Y1234 and/or Y1235 because of steric hindrance (*33*).

Dephosphorylation did not result in significant modulation of specific kinase activity of the different Met forms, which remained entirely consistent with those determined for untreated mutants, decreasing in the order: YYD > YYY > FYY > FYD. In particular, the activity of the completely dephosphorylated YYD was still slightly higher than that of the partially phosphorylated YYY. These data confirmed that the different activities are not related to the overall phosphorylation status of the proteins expressed in insect cells. They also showed that the Y1235D mutation can at least partially compensate for the loss of Y1235 phosphorylation in YYD and induce partial activation. Also, at a difference with YYY Met, this happens irrespective of the phosphorylation at Y1234. This effect is not observed when Y1194 is mutated to a phenylalanine, confirming the importance of an intact Y1194 for both the wild type and Y1235D mutant.

To understand how autophosphorylation modulates the specific activity of the proteins, we preincubated the dephosphorylated Met forms with ATP prior to the *in vitro* kinase assay. *In vitro* autophosphorylation of the dephosphorylated Met proteins resulted in the complete phosphorylation of virtually all Met forms (Table 1, group C). The YYY and FYY proteins were phosphorylated prevalently on two or more sites, with 2.1 and 2.6 phosphates/molecule, while the YYD and FYD mutants were predominantly di- and monophosphorylated, with 1.7 and 1.1 phosphates/molecule. In parallel, the specific activities of FYY and YYY increased 2−3-fold, while the YYD and FYD mutants were not activated by autophosphorylation.

Analysis of the different Met proteins by Western blotting using specific anti-pY1234/1235 antibodies revealed low levels of phosphorylation on Y1234 and/or Y1235 on Met proteins purified from insect cells, whereas one or both of these residues became highly phosphorylated in YYY and FYY after *in vitro* autophosphorylation (Figure 3B). The lack of detection by Western blot analysis of phosphorylation on Y1234 in the YYD mutant can be explained by the inability of the specific anti-pY1234/1235 antibodies to recognize the modified A loop containing the Y1235D substitution. Indeed, peptide mapping by MS showed Y1234 to be completely phosphorylated also in YYD and FYD after *in vitro* autophosphorylation (data not shown). In summary, *in vitro* autophosphorylation of Y1234−Y1235 results in full enzymatic activation of YYY and FYY proteins, irrespective of their initial phosphorylation state and activity, while the YYD and FYD mutants are not further activated by autophosphorylation on Y1234.

The inability to fully activate the YYD and FYD mutants despite their complete phosphorylation on Y1234 demonstrates that the Y1235D-activating mutation is not able to induce the same effect as two phosphotyrosines in the A loop (*14*−*16*). The capability of these mutants to preserve the signal transduction mediated by phosphorylation of the docking site was investigated using specific anti-pY1349 antibodies. Whereas Y1349 was highly phosphorylated in YYY, a faint phosphorylation of this site was observed in the FYY and YYD proteins purified from insect cells. In contrast, the levels of phosphorylated Y1349 increased significantly in all three forms after autophosphorylation (Figure 3C), suggesting that the Y1235D mutation can induce per se some degree of functional activation of its signal transduction site, which increases upon *in vitro* autophosphorylation.

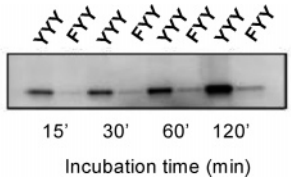

FIGURE 4: Comparison of the rates of autophosphorylation of YYY and FYY Met. The autophosphorylation assay was carried out at room temperature using 100 nM dephosphorylated YYY and FYY in 20 μL of kinase buffer containing [γ-^{32}P]ATP (2.5 μCi/sample) and 10 μM unlabeled ATP. The reaction was stopped at 15′, 30′, 60′ and 120′ by addition of 10 mM EDTA and Laemmli buffer. Reactions were analyzed using 10% SDS−PAGE and autoradiography of the dried gel.

Kinetics of Autophosphorylation. Phosphorylation of Y1194 was identified by mass spectrometry as a major phosphorylation site in YYY Met. Substitution of this residue seems to affect the basal specific activity of FYY purified from insect cells, but it does not hamper its full activation after *in vitro* autophosphorylation. To test whether this mutation may have affected the kinetics of activation, an autophosphorylation assay was performed in the presence of 10 μM ATP at room temperature using the FYY and YYY mutants at a concentration of 100 nM. Interestingly, in these conditions, FYY autophosphorylated at a substantially lower rate than YYY, and its level of autophosphorylation after 120 min was visibly lower than that observed after 15 min with YYY (Figure 4). Similar results were obtained at higher (1 μM) enzyme concentration (data not shown). However, under the conditions used for the *in vitro* autophosphorylation prior to the kinase assay (20−30 μM enzyme and 10 mM ATP at 37 °C), FYY was phosphorylated to the same extent as YYY (see Table 1, group C). These observations suggest that the Y1194F mutation could impair enzyme activity (see Table 1, group A) by significantly reducing kinase activation kinetics under physiological conditions.

Effect of the Mutations on the Binding of the Met Inhibitor K252a. K252a is a staurosporin analogue described as a potent inhibitor of Met kinase activity in cells (*34*). We used ITC to study the binding of K252a to phosphorylated and partially unphosphorylated YYY as well as the different Met mutants. In the structure of apo-Met FFD, residues D1228−Y1230 block the access of K252a to the active site (Figure S3 in the Supporting Information) and the comparison of the apo-crystal structure with the inhibitor cocrystal structure shows that these residues rearrange considerably to accommodate the ligand (*29*). Indeed, this is reflected in the

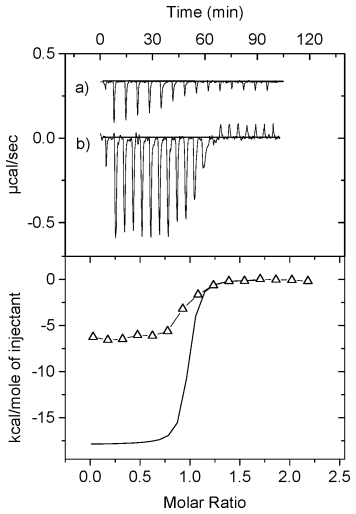

FIGURE 5: ITC binding study of the Met inhibitor K252a. The upper panel shows the raw heat data obtained over a series of injections of phosphatase-treated YYY Met (trace a) and FFD Met (trace b) into PBS buffer containing 8 μM K252a. The lower panel shows the integrated binding heats after subtraction of dilution heats (not shown) for FFD Met and phosphatase-treated YYY Met (△). The data obtained for the nonlinear least-squares fits are summarized in Table 2.

Table 2: ITC Data for the Binding of K525a to Met[a]

protein[b]	K_D (μM)	K_B (10^7 M^{-1})	ΔH^{obs} (kcal mol^{-1})	$T\Delta S^{obs}$ (kcal mol^{-1})	ΔG^{obs} (kcal mol^{-1})	N[c]
YYY	0.063	1.6 ± 0.3	-7.0 ± 0.1	2.6	−9.6	0.82
YYY*	0.062	1.6 ± 0.4	-6.5 ± 0.1	3.2	−9.7	0.90
FYY	0.053	1.8 ± 0.8	-5.6 ± 0.2	4.1	−9.7	0.95
YYD	0.050	2.0 ± 0.4	-6.0 ± 0.2	3.8	−9.8	1.10
FYD	0.014	7.2 ± 1.2	-5.7 ± 0.2	4.8	−10.5	0.98
FYD**	0.040	2.5 ± 0.8	-9.7 ± 0.2	0.3	−10.0	0.80
FFD	0.011	9.3 ± 2.0	-18.2 ± 0.2	−7.5	−10.7	0.94

[a] Errors given in the table are errors of the nonlinear least-squares fit only. [b] All Met forms were analyzed directly after purification from insect cells (Table 1, group A) with the exception of YYY* that was partially dephosphorylated (Table 1, group B) and FYD** that was subjected to *in vitro* autophosphorylation (Table 1, group C). [c] N = experimentally determined stoichiometry of the interaction.

considerably large binding enthalpy change measured for the FFD mutant ($\Delta H^{obs} = -18.2 \pm 0.2$ kcal/mol) upon binding of K525a (Figure 5). Much smaller binding enthalpies were observed for YYY as well as the FYD and FYY mutants, suggesting that these proteins do not undergo such drastic structural changes upon inhibitor binding (Figure 5 and Table 2). Interestingly, both the FFD and FYD mutants bound K252a with about 4−5-fold higher affinity than YYY and FYY. To analyze if there was a correlation between the higher level of phosphorylation of YYY and FYY with respect to the other mutants (Table 1, group A) and their lower affinity for the inhibitor, we repeated the ITC measurement using the phosphatase-treated YYY (Table 1, group B). However, after this treatment, no change in the affinity for K252a was observed, which might be due to only partial dephosphorylation of Y1234. In contrast, *in vitro* autophosphorylation of FYD, which we previously showed to occur mainly at position 1234, resulted in a 3-fold lower affinity of Met for K252a when compared to the unphosphorylated mutant as well as in a larger, more favorable, binding enthalpy change (Table 2), suggesting that phosphorylation at Y1234 may play a role in inhibitor binding by modulation of A-loop flexibility.

DISCUSSION

The molecular mechanism for activation of wild-type and mutated Met has been extensively studied using cell-based assays and semiquantitative biochemical approaches based on immunoprecipitation of Met proteins from mammalian cells, coupled to immunological detection of protein phosphorylation (*19*, *28*, *35*). Recently, transient expression in COS cells coupled to Western blotting with selective anti-pTyr antibodies was used to study in depth the mechanism of activation of wild type and Met mutants D1228H, D1228N, and M1250T (*28*).

Here, we report the use of >90% pure, extensively characterized proteins produced in insect cells coupled to quantitative approaches to analyze protein phosphorylation and enzymatic activity, as a very robust approach to analyze in depth the importance of individual residues and their phosphorylation state for Met enzymatic activity. Using limited proteolysis and mass spectrometry, we were able to identify a compact domain of Met that could be expressed at significant levels as a soluble, nonaggregated, active protein. Because of very high levels of expression, exogenous RTKs produced either in insect cells or in mammalian COS cells undergo spontaneous clusterization and trans-autophosphorylation (*28*). As described for COS cells, recombinant wild-type Met from insect cells was highly phosphorylated at several sites, including Y1234 and Y1235. When we attempted to modulate its activity by *in vitro* dephosphorylation, it proved to be technically very difficult to obtain a nonphosphorylated form even by prolonged phosphatase treatment. Phosphomapping of the YYY Met kinase domain expressed in insect cells enabled us to identify three major phosphorylation sites; the well-known tyrosine doublet Y1234 and Y1235 on the A loop (*14*−*16*) and Y1194 in the hinge region, whose phosphorylation had not been previously reported. To study the function of these three tyrosine residues and possibly produce a nonphosphorylated, active form suitable for structural studies, we generated combinations of silencing (from Tyr to Phe) mutations on Y1194 and/or Y1234 and the naturally occurring phosphotyrosine mimetic mutation Y1235D. We then characterized the different proteins by a combination of mass spectrometry, phosphospecific antibodies, and enzymatic assays.

Major differences were observed in the phosphorylation state of the mutants purified from insect cells, which, because they were produced under very similar conditions and with comparable yields, would not seem to be due to the effect of endogenous kinases but rather to intrinsic autophosphorylation properties of the different forms, as well as the presence of the major phosphorylatable sites.

Interestingly, our studies demonstrated little correlation between the overall degree of phosphorylation and specific activity of Met and its mutants. Instead, in accordance with previous observations (*14*, *15*, *28*), for wild-type Met, the activity depended upon the degree of the specific phosphorylation of Y1234 and Y1235. To obtain a constitutively active mutant, we introduced the Y1235D mutation that should mimic the phosphorylated tyrosine at this position, by analogy with what has been proposed to explain the

activation of B-Raf, having aspartic acid at the corresponding position (*36*). Biological studies indicate that this naturally occurring mutation leads to constitutive Met activation (*25*, *26*), and a qualitative analysis showed its association with higher *in vitro* kinase activity with respect to the wild type (*26*). In agreement with these data, we found that the YYD mutant purified from insect cells has a basal activity superior to that of YYY Met.

For wild-type Met, it has been suggested that Y1235 may be the first phosphorylation event, which would not be sufficient to release auto-inhibition until a second phosphorylation event occurs on Y1234 (*28*). In depth biochemical characterization of the D1228H/N and M1250T mutants showed that these proteins are not phosphorylated on Y1234 yet retain full kinase activity (*28*). Moreover, mutagenesis of Y1234 does not affect the biochemical or biological function of these mutants. In contrast, Y1234 of the Y1235D mutant is still capable of becoming phosphorylated *in vitro*. However, phosphorylation of Y1234 does not seem to contribute to the activation of the Y1235D mutant. In fact, its activity is neither affected by complete dephosphorylation upon phosphatase treatment nor increased after *in vitro* incubation with ATP, which we found by mass spectrometry to induce Y1234 phosphorylation. On the other hand, *in vitro* incubation of YYY results in higher activity compared to YYD, suggesting that the mutation Y1235D triggers partial activation but cannot fully compensate a phosphorylated tyrosine at this position. Moreover, it is worth mentioning that *in vitro* incubation with ATP was found to increase phosphorylation at Y1349 both in YYY and YYD proteins; therefore, dimerization following receptor activation *in vivo* may still be able to increase the biological response of this mutated Met.

On the basis of these results, we conclude that the constitutive activation of the Y1235D mutant differs from the molecular mechanisms of other oncogenic mutations, such as D1228H/N and M1250T, which overcome the need for the second phosphorylation step on Y1234 by reducing the threshold for activation but can only display their oncogenic potential upon stimulation with HGF (*28*, *37*).

The capability of the Y1235D mutant to uncouple kinase activation from ligand binding may very well explain the ability of this type of mutation to induce metastatic properties also in carcinoma cell lines not expressing HGF (*26*). However, it is noteworthy that the Y1235D Met mutant overexpressed in human carcinoma cell lines can be further stimulated by HGF stimulation (*26*). On the basis of our data, the oncogenic phenotype observed with this mutant *in vivo* may be due to a sustained phosphorylation at the 1349−1356 signaling site rather than further activation of the kinase. Thus, constitutive activation, rather than increased kinase activity, seems to be the key explanation for the oncogenic potential of this mutation.

In this study, we also identified Y1194 as a major phosphorylation site in recombinant Met that had not been previously described. The biological role of this residue is still not fully understood. However, the Y1194F mutation has been shown to significantly diminish mitogenic signaling and invasive properties of oncogenic Met in response to HGF (*30*). In addition, mutation of the homologous residue in the Ret-oncogene affects the transforming activity of this protein (*38*). This residue is highly conserved among receptor tyrosine kinases (nearly 90%) and strictly conserved among the closest relatives of Met, including RET, RON, insulin receptor kinase, IGF1R, and FGFR (*29*, *35*, *39*, *40*). This region is also structurally conserved (*29*), with the hydroxyl group of Y1194 most likely forming a triad hydrogen bond with D1133 and S1135 in the wild-type Met (*30*), similar to the interactions observed in the insulin receptor (*31*) and other RTKs, such as IGF1R and FGFR. In Met FFD mutant, hydrogen bonds formed by the tyrosine hydroxyl group are disrupted and F1194 sits in a hydrophobic pocket formed by K1198, L1195, H1136, and F1134 (Figure 6), although the local environment of Y1194 is conserved in the crystal structure (*29*). Currently, there is no evidence that Y1194 needs to be phosphorylated or that this site is indeed phosphorylated *in vivo*. However, phosphorylation of Y1194 will induce new noncovalent interactions in this region that are possibly coupled to structural rearrangements of the two kinase lobes. It is therefore very likely that modulations close to the hinge of the lobes at Y1194 play an important role in the overall flexibility of Met and influence its activation kinetics. The effect of the Y1194F mutation is also observed in the presence of the activating mutation Y1235D, resulting in a limitation of its potential activity. This finding underlines the importance of a free tyrosine in this position. Moreover, our results suggest that the slow activation kinetics observed could elicit an increased threshold for Met signaling in cells, which could account for the aberrant physiological function of Met (*30*) and possibly Ret (*38*) mutated at this residue. More work will be needed to understand if this residue is phosphorylated *in vivo* in Met and other receptor tyrosine kinases.

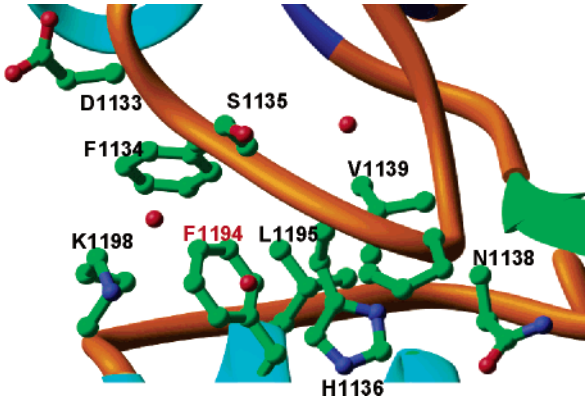

FIGURE 6: Structure of the region encompassing the highly conserved 1194 residue in the FFD mutant. In the crystal structure of the FFD mutant, F1194 sits in a hydrophobic pocket formed by F1134, H1136, L1195, and K1198 (*29*). The orientation of this residue is conserved, indicating that the mutation does not alter the protein structure in this region. However, in the absence of the phenylhydoxyl group, the mutant is unable to form hydrogen bonds with the neighboring residues D1133 and S1135.

Analysis of the FFD mutant in complex with the K252a mutant showed interactions of the N-terminal residues of the A loop with the inhibitor (*29*). We then applied ITC to study the interactions of the FFD mutant in parallel with the other Met proteins. The large binding enthalpy change measured for the FFD mutant ($\Delta H^{obs} = -18.2 \pm 0.2$ kcal/mol) indicates that binding of K252a induces conformational changes in this mutant (*29*, Figure 5). In contrast, binding enthalpy values were considerably smaller for YYY, YYD, FYD, and FYY Met, suggesting that structural rearrange-

ments do not take place to the same extent upon binding of K252a to these proteins.

One interesting aspect of the thermodynamic data that we obtained is that, even though binding constants of K252a to the Met mutants are similar, the thermodynamic driving forces that give rise to the binding are very different. K252a binding to FFD is strongly favored by enthalpy changes (ΔH^{obs}) and opposed by entropy changes (ΔS^{obs}), whereas unphosphorylated FYD binds K252a with similar affinity but with a favorable entropy change and a significantly reduced enthalpy contribution to binding. Such data gives interesting insights into the biophysical reasons of inhibitor recognition that can be used to support structure-based drug-design efforts. Interestingly, binding studies with K252a also showed that phosphorylation of Y1234 influences inhibitor binding and modulates inhibitor binding thermodynamics. Because of the low affinity for ATP, we were unable to unambiguously demonstrate any correlation between phosphorylation of Y1234 and lower affinity for ATP, but it is conceivable that phosphorylation of this site influences the affinities for ATP. Indeed, it was shown by Morotti et al. (*34*) that K252a was more potent on another mutated form of Met (M1250T) than on the wild type. Because the Y1235D mutation has been identified in several metastases, it is interesting to speculate that the mutated Met form found in some tumors may be more sensitive to staurosporin-like inhibitors than Met activated under physiological conditions, opening new possibilities in the design of specific inhibitors against oncogenic Met.

Recently, it was reported that the Met kinase inhibitor SU11274 differentially affects the activity and signaling of various mutant forms of Met (*42*). The Met mutations M1250T and H1094Y were potently inhibited, while the L1195V and Y1230H variants were found to be resistant to this compound both in terms of phosphorylation and downstream signaling. Interestingly, it has also been recently reported that individual Met mutations induce different tumor types in mice (*43*). When these data are taken together, they suggest that the effects of individual mutations on Met tyrosine kinase activation and signaling, as well as their impact on Met pharmacological inhibition, need to be investigated on a case by case basis.

In support of the new concept of selective drug discovery, the L858R mutation in EGFR in patients with lung carcinoma was demonstrated to render them more sensitive to gefitinib treatment (*44*). This suggests that a detailed genetic analysis of individual tumors will be a necessary prerequisite for the success of targeted therapy. The analysis of various colorectal cancer samples showed the presence of point mutations in different branches of the tyrosine "kinome" in a minimum of 30% of the investigated cases (*45*). Mutations have also emerged as a major cause of tumor resistance to the Gleevec Abl inhibitor, and this may be a common mechanism of escape from treatment with kinase inhibitors (*46*). Thus, for the design of kinase inhibitors as anticancer drugs, the effects of spontaneous and induced mutations on the target activation and drug binding need to be considered for a successful therapy.

ACKNOWLEDGMENT

We thank Paolo Caccia for his contribution during the initial phase of this work, Al Stewart for continuous encouraging support, Michael Forstner for useful discussion, and Maria Flocco for support. We also thank Rosario Baldi and Silvia Messali for technical support and Jan Malyszko, Cristiana Marcozzi, and Sonia Troiani for their contribution. C. C. is grateful to Graziella Bisconti Cristiani for personal support.

SUPPORTING INFORMATION AVAILABLE

Figure S1, MALDI mass spectrum of wild-type Met phosphopeptides; Figure S2, CD spectra of wild-type and mutant Met proteins; Figure S3, residues of the A loop of FFD apo-Met and in complex with K252a. This material is available free of charge via the Internet at http://pubs.acs.org.

REFERENCES

1. Bottaro, D. P., Rubin, J. S., Faletto, D. L., Chan, A. M., Kmiecik, T. E., Vande Woude, G. F., and Aaronson, S. A. (1991) Identification of the hepatocyte growth factor receptor as the c-Met proto-oncogene product, *Science 251*, 802−804.
2. Park, M., Dean, M., Cooper, C. S., Schmidt, M., O'Brien, S. J., Blair, D. G., and Vande Woude, G. F. (1986) Mechanism of Met oncogene activation, *Cell 45*, 895−904.
3. Comoglio, P. M., and Trusolino, L. (2002) Invasive growth: From development to metastasis, *J. Clin. Invest. 109*, 857−862.
4. Maulik, G., Shrikhande, A., Kijima, T., Ma, P. C., Morrison, P. T., and Salgia, R. (2002) Role of the hepatocyte growth factor receptor, c-Met, in oncogenesis and potential for therapeutic inhibition, *Cytokine Growth Factor Rev. 13*, 41−59.
5. Di Renzo, M. F., Olivero, M., Katsaros, D., Crepaldi, T., Gaglia, P., Zola, P., Sismondi, P., and Comoglio, P. M. (1994) Overexpression of the Met/HGF receptor in ovarian cancer, *Int. J. Cancer 58*, 658−662.
6. Matsumoto, K., Matsumoto, K., Nakamura, T., and Kramer, R. H. (1994) Hepatocyte growth factor/scatter factor induces tyrosine phosphorylation of focal adhesion kinase (p125FAK) and promotes migration and invasion by oral squamous cell carcinoma cells, *J. Biol. Chem. 269*, 31807−31813.
7. Trusolino, L., Serini, G., Cecchini, G., Besati, C., Ambesi-Impiombato, F. S., Marchisio, P. C., and De Filippi, R. (1998) Growth factor-dependent activation of $\alpha v\beta 3$ integrin in normal epithelial cells: Implications for tumor invasion, *J. Cell Biol. 142*, 1145−1156.
8. Jeffers, M., Rong, S., and Vande Woude, G. F. (1996) Enhanced tumorigenicity and invasion-metastasis by hepatocyte growth factor/scatter factor-Met signalling in human cells concomitant with induction of the urokinase proteolysis network, *Mol. Cell. Biol. 16*, 1115−1125.
9. Cohen, P. (2002) Protein kinases—The major drug targets of the twenty-first century? *Nat. Rev. Drug Discovery 1*, 309−315.
10. Furge, K. A., Kiewlich, D., Le, P., Vo, M. N., Faure, M., Howlett, A. R., Lipson, K. E., Woude, G. F., and Webb, C. P. (2001) Suppression of Ras-mediated tumorigenicity and metastasis through inhibition of the Met receptor tyrosine kinase, *Proc. Natl. Acad. Sci. U.S.A. 98*, 10722−10727.
11. Michieli, P., Mazzone, M., Basilico, C., Cavassa, S., Sottile, A., Naldini, L., and Comoglio, P. M. (2004) Targeting the tumor and its microenvironment by a dual-function decoy Met receptor, *Cancer Cell 6*, 61−73.
12. Weiss, A., and Schlessinger, J. (1998) Switching signals on or off by receptor dimerization, *Cell 94*, 277−280.
13. Kong-Beltran, M., Stamos, J., and Wickramasinghe, D. (2004) The Sema domain of Met is necessary for receptor dimerization and activation, *Cancer Cell 6*, 75−84.
14. Ferracini, R., Longati, P., Naldini, L., Vigna, E., and Comoglio, P. M. (1991) Identification of the major autophosphorylation site of the Met/hepatocyte growth factor receptor tyrosine kinase, *J. Biol. Chem. 266*, 19558−19564.
15. Longati, P., Bardelli, A., Ponzetto, C., Naldini, L., and Comoglio, P. M. (1994) Tyrosines 1234−1235 are critical for activation of the tyrosine kinase encoded by the Met proto-oncogene (HGF receptor), *Oncogene 9*, 49−57.
16. Ponzetto, C., Bardelli, A., Zhen, Z., Maina, F., dalla Zonca, P., Giordano, S., Graziani, A., Panayotou, G., and Comoglio, P. M. (1994) A multifunctional docking site mediates signaling and

transformation by the hepatocyte growth factor/scatter factor receptor family, *Cell 77*, 261−271.
17. Fixman, E. D., Fournier, T. M., Kamikura, D. M., Naujokas, M. A., and Park, M. (1996*)* Pathways downstream of Shc and Grb2 are required for cell transformation by the Tpr-Met oncoprotein, *J. Biol. Chem. 271*, 13116−13122.
18. Maina, F., Pantè, G., Helmbacher, F., Andres, R., Porthin, A., Davies, A. M., Ponzetto, C., and Klein, R. (2001) Coupling Met to specific pathways results in distinct developmental outcomes, *Mol. Cell 7*, 1293−1306.
19. Maritano, D., Accornero, P., Bonifaci, N., and Ponzetto, C. (2000) Two mutations affecting conserved residues in the Met receptor operate via different mechanisms, *Oncogene 19*, 1354−1361.
20. Schmidt, L., Duh, F. M., Chen, F., Kishida, T., Glenn, G., Choyke, P., Scherer, S. W., Zhuang, Z., Lubensky, I., Dean, M., Allikmets, R., Chidambaram, A., Bergerheim, U. R., Feltis, J. T., Casadevall, C., Zamarron, A., Bernues, M., Richard, S., Lips, C. J., Walther, M. M., Tsui, L. C., Geil, L., Orcutt, M. L., Stackhouse, T., and Zbar, B. (1997) Germline and somatic mutations in the tyrosine kinase domain of the Met proto-oncogene in papillary renal carcinomas, *Nat. Genet. 16*, 68−73.
21. Olivero, M., Valente, G., Bardelli, A., Longati, P., Ferrero, N., Cracco, C., Terrone, C., Rocca-Rossetti, S., Comoglio, P. M., and Di Renzo, M. F. (1999) Novel mutation in the ATP-binding site of the Met oncogene tyrosine kinase in a HPRCC family, *Int. J. Cancer 82*, 640−643.
22. Lee, J.-H, Han, S.-U., Cho, H., Jennings, B., Gerrard, B., Dean, M., Schmidt, L., Zbar, B., and Vande Woude, G. F. (2000) A novel germ line juxtamembrane Met mutation in human gastric cancer, *Oncogene 19*, 4947−4953.
23. Schmidt, L., Junker, K., Nakaigawa, N., Kinjerski, T., Weirich, G., Miller, M., Lubensky, I., Neumann, H. P., Brauch, H., Decker, J., Vocke, C., Brown, J. A., Jenkins, R., Richard, S., Bergerheim, U., Gerrard, B., Dean, M., Linehan, W. M., and Zbar, B. (1999) Novel mutations of the Met proto-oncogene in papillary renal carcinomas, *Oncogene 18*, 2343−2350.
24. Park, W. S., Dong, S. M., Kim, S. Y., Na, E. Y., Shin, M. S., Pi, J. H., Kim, B. J., Bae, J. H., Hong, Y. K., Lee, K. S., Lee, S. H., Yoo, N. J., Jang, J. J., Pack, S., Zhuang, Z., Schmidt, L., Zbar, B., and Lee, J. Y. (1999) Somatic mutations in the kinase domain of the Met/hepatocyte growth factor receptor gene in childhood hepatocellular carcinomas, *Cancer Res. 59*, 307−310.
25. Di Renzo, M. F., Olivero, M., Martone, T., Maffe, A., Maggiora, P., Stefani, A. D., Valente, G., Giordano, S., Cortesina, G., and Comoglio, P. M. (2000) Somatic mutations of the Met oncogene are selected during metastatic spread of human HNSC carcinomas, *Oncogene 19*, 1547−1555.
26. Lorenzato, A., Olivero, M., Patanè, S., Rosso, E., Oliaro, A., Comoglio, P. M., and Di Renzo, M. F. (2002) Novel somatic mutations of the Met oncogene in human carcinoma metastases activating cell motility and invasion, *Cancer Res. 62*, 7025−7030.
27. Miller, M., Ginalski, K., Lesyng, B., Nakaigawa, N., Schmidt, L., and Zbar, B. (2001) Structural basis of oncogenic activation caused by point mutations in the kinase domain of the Met proto-oncogene: Modeling studies, *Proteins 44*, 32−43.
28. Chiara, F., Micheli, P., Pugliese, L., and Comoglio, P. (2003) Mutations in the Met oncogene unveil a "dual switch" mechanism controlling tyrosine kinase activity, *J. Biol. Chem. 278*, 29352−29358.
29. Schiering, N., Knapp, S., Marconi, M., Flocco, M., Cui, J., Perego, R., Rusconi, L., and Cristiani, C. (2003) Crystal structure of the tyrosine kinase domain of the hepatocyte growth factor receptor c-Met and its complex with the microbial alkaloid K-252a, *Proc. Natl. Acad. Sci. U.S.A. 100*, 12654−12659.
30. Jeffers, M., Koochekpour, S., Fiscella, M., Sathyanarayana, B. K., and Vande Woude, G. F. (1998) Signaling requirements for oncogenic forms of the Met tyrosine kinase receptor, *Oncogene 17*, 2691−2700.
31. Sreerama, N., Venyaminov, S. Y., and Woddy, R. W. (1999) Estimation of the number of α-helical and *β*-strand segments in proteins using circular dichroism spectroscopy, *Protein Sci. 8*, 370−380.
32. Philo, J. S. (2000) A method for directly fitting the time derivative of sedimentation velocity data and an alternative algorithm for calculating sedimentation coefficient distribution functions, *Anal. Biochem. 279*, 151−163.
33. Kamikura, D. M., Naujokas, M. A., and Park, M. (1996) Identification of tyrosine 489 in the carboxy terminus of the Tpr-Met oncoprotein as a major site of autophosphorylation, *Biochemistry 35*, 1010−1017.
34. Morotti, A., Mila, S., Accornero, P., Tagliabue, E., and Ponzetto, C. (2002) K252a inhibits the oncogenic properties of Met, the HGF receptor, *Oncogene 21*, 4885−4893.
35. Jeffers, M., Schmidt, L., Nakaigawa, N., Webb, C. P., Weirich, G., Kishida, T., Zbar, B., and Vande Woude, G. F. (1997) Activating mutations for the Met tyrosine kinase receptor in human cancer, *Proc. Natl. Acad. Sci. U.S.A. 94*, 11445−11450.
36. Marais, R., Light, Y., Paterson, H. F., Mason, C. S., and Marshall, C. J. (1997) Differential regulation of Raf-1, A-Raf, and B-Raf by oncogenic ras and tyrosine kinases, *J. Biol. Chem. 272*, 4378−4383.
37. Michieli, P., Basilico, C., Pennacchietti, S., Maffe, A., Tamagnone, L., Giordano, S., Bardelli, A., and Comoglio, P. M. (1999) Mutant Met-mediated transformation is ligand-dependent and can be inhibited by HGF antagonists, *Oncogene 18*, 5221−5231.
38. Iwashita, T., Asai, M., Murakami, H., Matsuyama, M., and Takahashi, M. (1996) Identification of tyrosine residues that are essential for transforming activity of the ret proto-oncogene with MEN2A or MEN2B mutation, *Oncogene 12*, 481−487.
39. Hanks, S. K. (1991) Eukaryotic protein kinases, *Curr. Opin. Struct. Biol. 1*, 369−383.
40. Hanks, S. K., and Quinn, A. M. (1991) Protein kinase catalytic domain sequence database: Identification of conserved features of primary structure and classification of family members, *Methods Enzymol. 200*, 38−62.
41. Hubbard, S. R., Wei, L., Ellis, L., and Hendrickson, W. A. (1994) Crystal structure of the tyrosine kinase domain of the human insulin receptor, *Nature 372*, 746−754.
42. Berthou, S., Aebersold, D. M., Schmidt, L. S., Stroka, D., Heigl, C., Streit, B., Stalder, D., Gruber, G., Liang, C., Howlett, A. R., Candinas, D., Greiner, R. H., Lipson, K. E., and Zimmer, Y. (2004) The Met kinase inhibitor SU11274 exhibits a selective inhibition pattern toward different receptor mutated variants, *Oncogene 23*, 5387−5393.
43. Graveel, C., Su, Y., Koeman, J., Wang L.-M., Tessarollo, L., Fiscella, M., Birchmeier, C., Swiatek, P., Bronson, R., and Vande Woude, G. (2004) Activating Met mutations produce unique tumor profiles in mice with selective duplication of the mutant allele, *Proc. Natl. Acad. Sci. U.S.A. 101*, 17198−17203.
44. Paez, J. G., Janne, P. A., Lee, J. C., Tracy, S., Greulich, H., Gabriel, S., Herman, P., Kaye, F. J., Lindeman, N., Boggon, T. J., Naoki, K., Sasaki, H., Fujii, Y., Eck, M. J., Sellers, W. R., Johnson, B. E., and Meyerson, M. (2004) EGFR mutations in lung cancer: Correlation with clinical response to gefitinib therapy, *Science 304*, 1497−500.
45. Bardelli, A., Parsons, D. W., Silliman, N., Ptak, J., Szabo, S., Saha, S., Markowitz, S., Willson, J. K., Parmigiani, G., Kinzler, K. W., Vogelstein, B., and Velculescu, V. E. (2003) Mutational analysis of the tyrosine kinome in colorectal cancers, *Scienc*e *300*, 949.
46. Cowan-Jacob, S. W., Guez, V., Fendrich, G., Griffin, J. D., Fabbro, D., Furet, P., Liebetanz, J., Mestan, J., and Manley, P. W. (2004) Imatinib (STI571) resistance in chronic myelogenous leukemia: Molecular basis of the underlying mechanisms and potential strategies for treatment, *Mini Rev. Med. Chem. 4*, 285−299.

BI051242K